Signal Processing and Renewable Energy
March 2021, (pp. 79-95)
ISSN: 2588-7327
eISSN: 2588-7335

HVDC Line Model for Load Frequency Control Using Harmony Search Algorithm Application

Mohammadali Shahab[1,2], Ghazanfar Shahgholian[1,2*]

[1] Department of Electrical Engineering, Najafabad Branch, Islamic Azad University, Najafabad, Iran.
[2] Smart Microgrid Research Center, Najafabad Branch, Islamic Azad University, Najafabad, Iran.

Received: 16-Nov-2020, Revised: 25-Nov-2020, Accepted: 01-Dec-2020.

Abstract

Load frequency control (LFC) is used as part of automatic generation control (AGC) in power systems. LFC with the automatic voltage regulator (AVR) plays an important role in maintaining the frequency and constant voltage. In this paper, a method for load frequency control in reconstructed electrical systems using high voltage direct current (HVDC) line is presented. An accurate and complete model based on the control circuit and equations with HVDC controller design is considered and its parameters are optimized using the harmony search algorithm (HAS). To test the method, the power system is simulated with three-area. The simulation results show the proper performance of the power system against sudden load changes and disturbances caused by other areas.

Keywords: High Voltage Direct Current, Harmony Search Algorithm, Load Frequency Control.

1. INTRODUCTION

With the development of power systems and especially the development of energy consumption, an important issue in the electricity industry is the power supply under constant voltage and frequency [1-4].

Load-frequency control (LFC) is one of the important subjects of electric power systems [5,6]. The objectives of load frequency control are to maintain power balance between interconnected areas and to control the power flow in the tie-lines [7]. So far, various studies have been conducted on

*Corresponding Authors Email: shahgholian@iaun.ac.ir

the application of LFC in the power system [8].

A review of different controllers utilized in traditional as well as a renewable energy-based power system for load frequency management (LFM) such as; classical controllers, sliding mode controller (SMC), fractional order-controllers, cascaded controllers, H-infinity controller, tilt-integral-derivative controllers and other recently developed controllers is presented in [9].

An overview of the different types of unregulated power system structures, market models, contract agreements, and different control methods/techniques to reduce the various LFC issues in an unregulated power system is provided in [10], which the detailed analysis of various control methodologies based on classical control, robust and self-tuning control and various soft computing control techniques are discussed.

A model to control the frequency of the wind farm connected to conventional units is presented in [11], which is conducted to improve the efficiency of the model, the defined frequency control parameters are optimized based on a multi-objective function using PSO algorithm.

An optimal method to tune the PID controller for a hydraulic turbine coupled with the corresponding TDC is presented in [12], which the problem consists of adjusting both the parameters of the controller and compensator such as the time response and remains close to the specified one.

Energy transmission by HVDC is known as the effective solution to control load-frequency that can optimize the system damping and controlling the frequency oscillation in the power system [13,14]. In the AC-DC transmission system, a dc system can be used to optimize the transient stability in an emergency and to optimize the frequency stability at a steady state. The ability of the dc system to control is very quick [15,16].

Recent advances in power electronics have led to the expansion of HVDC links and renewable-based generation in power systems. So far, various studies have been conducted in the field of frequency control in the HVDC interconnected systems [17,18].

A complete state-space mathematical model of multi area ac/dc interconnected LFC system with phase-locked loop and time delay is presented in [19], which a Pade approximation method used for adding the effects of communication delays on AGC operation and the state-space models.

A survey on LFC mechanism is presented in [20], which reveals the investigation of soft computing based optimization technique and application of ESS and HVDC-link in LFC. Also, the different control techniques of LFC are mentioned, which include all the recent application of FACTS devices.

The accurate modeling of HVDC links for the dynamic studies of automatic generation control/LFC of the multi-area interconnected power system is presented in [21], in which the comparative analysis has been performed to demonstrate error being accrued due to the use of the conventional model of HVDC links.

To enhance load frequency control and automatic generation control, a HVDC tie-line based on a simple first-order transfer function is modeled, and proposed for the multi-area interconnected power system in [22].

An improved ant colony optimization algorithm optimized fuzzy PID controller for load frequency control of multi area systems is proposed in [23], and a modified objective function using to improve the performance of the controller.

In this paper, a model based on the circuit and controlling equation of the HVDC line is presented. This model compensates for the shortcomings of previous models to check frequency control. This model investigates in a power system three-area. A harmonic search algorithm is used to optimize the controller parameters. Finally, the effectiveness of the proposed controller with the proposed method is evaluated by time-domain simulations in MATLAB/Simulink environment. The rest of this paper is organized as follows. The mathematical model of the study system is described in Section 2. The detailed description of HSA is presented in Section 3. Simulation results are presented in Section 4 to verify the effectiveness of the proposed method. Conclusions are drawn in Section 5.

2. MATHEMATICAL MODEL OF THE STUDY SYSTEM

The power system is a typical nonlinear differential algebraic system [24,25]. The differential or state equations describe the system dynamic including generators, motors, governors, HVDC, FACTs and their controllers [26-28]. The equal circuit of the system for a DC line with line commutation is shown in Fig. 1.

Usually, dc converters have four controlling modes which are included of [29,30]: constant current, constant power, constant α or constant γ and constant dc voltage.

In most cases, rectifier converter operates in constant current mode and inverter converter operates in constant extinction angle mode [31, 32]. In other words, the rectifier maintains a constant current (CC) and the inverter maintains a sufficient discharge margin, which operates at a constant extinction angle (CEA) [33,34].

Inverter specification can be moved up or down by changing the transformer tap converter. While the tap converter is moving, the CEA regulator provides the desired γ immediately.

As a result, the direct current is changed that returns to the desired value by the aid of rectifier current regulator [35,36]. In practice, depending on the current regulator, constant current specification may not be vertical. In this case, as it will be shown further, this specification will become high negative slope because of limit gain of the current regulator. With a K regulator gain, we have (Fig. 2):

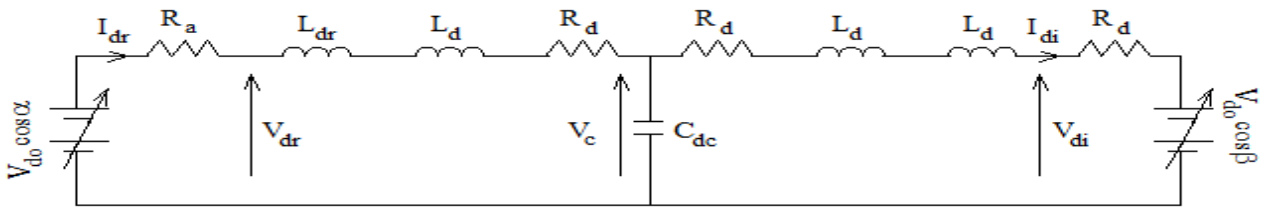

Fig. 1. System equal circuit .

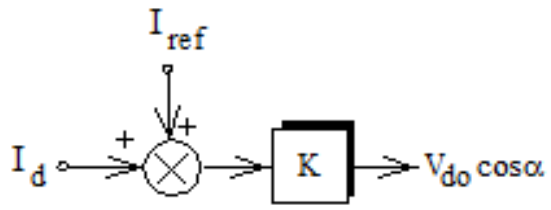

Fig. 2. Current regulator.

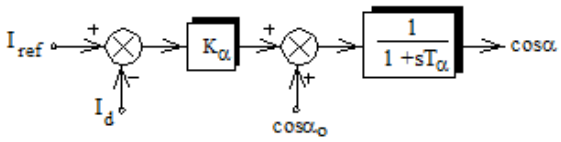

Fig. 3. Rectifier controller.

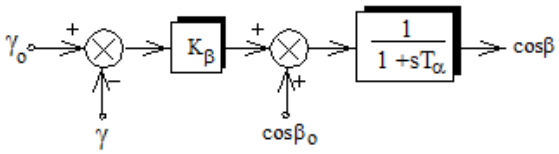

Fig. 4. Inverter controller.

$$V_{d0}\cos(\alpha) = K(I_{ref} - I_d) = V_d + R_{cr} I_d \quad (1)$$

$$\frac{\Delta V_d}{\Delta I_d} = -(K + R_{cr}) \quad (2)$$

CC specification becomes vertical completely with proportional regulator and by adding regulator as Fig. 3. Because this task is led to reduce the current error in steady-state mode and the current becomes constant. The same design helps us to control the rectifier in constant current mode.

Therefore:

$$T_\alpha \frac{d}{dt}(\cos\alpha) = -\cos(\alpha) + \cos(\alpha_o) + k_\alpha (I_{ref} - I_d) \quad (3)$$

Usually, the converter deviated around operation point in constant current mode, thus the nonlinear equation can become linear:

$$T_\alpha \frac{d}{dt}(1+\Delta\alpha) = -(1+\Delta\alpha) + (1+\Delta\alpha_0) + k_\alpha (I_{ref} - I_d) \quad (4)$$

$$T_\alpha \frac{d\alpha}{dt} = -\alpha + \alpha_o + k_\alpha (I_{ref} - I_d) \quad (5)$$

About constant extinction angle mode of inverter and according to Fig. 4, we will have the following relationship:

$$T_\beta \frac{d}{dt}\cos(\beta) = k_\beta(\gamma_0 - \gamma) + \cos\beta_o - \cos\beta \quad (6)$$

Therefore, the state equations for the converters are as follows:

$$\frac{d}{dt}\alpha = \frac{1}{T_\alpha}[-\alpha + \alpha_0 + k_\alpha u_\alpha(t)] \quad (7)$$

$$\frac{d}{dt}\beta = \frac{1}{T_\beta}[-\beta + \beta_0 - k_\beta u_\beta(t)] \quad (8)$$

where α and β are same angle of fire and ignition advance of rectifier and inverter, u_α and u_β are controlling inputs for adjusting α and β. According to the Fig. 1, V_d and P_{dc} are as follows:

$$V_d = V_{d0i}\cos(\beta) - R_C I_d \quad (9)$$

$$P_{dc} = V_{dc} I_{dc} \quad (10)$$

where α_o and β_o are primary adjusting values of regulator and T_α, T_β, k_α and k_β are controlling parameters of dc line and I_{ref} and

γ_o are current source values and extinction angle.

According to this equations, the dc line modeling in Matlab/Simulink software are performed. Equations also have been simulated as the Figs. 5 and 6.

If the frequency error increases, frequency of area 1 increases or frequency of area 2 decreases, more power must be transmitted from area 1 to area 2. Therefore, the values of the rectifier current source and the inverter extinction angle must be increased to transfer more power that increases the frequency error.

Finally, rectifier current source value and inverter extinction angle shall be reduced to transmit the more power from area 2 to area 1 and frequency error will be reduced.

In addition, the power fluctuations must be the same, so in addition to the frequency error, the line power error must also be considered.

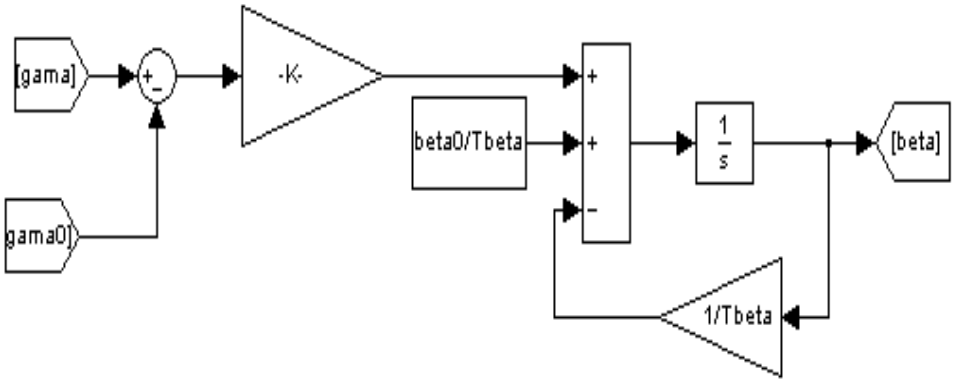

Fig. 5. Placing equations (7) and (8) in Matlab/Simulink environment.

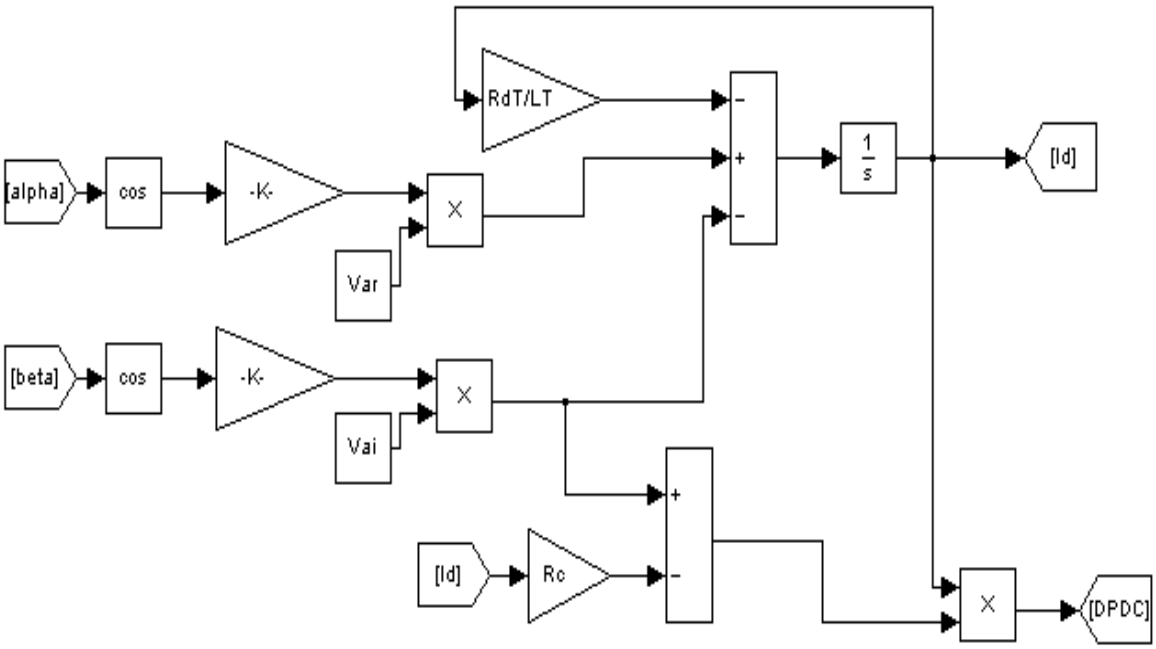

Fig. 6. Placing the equations (9) and (10) in Matlab/Simulink environment.

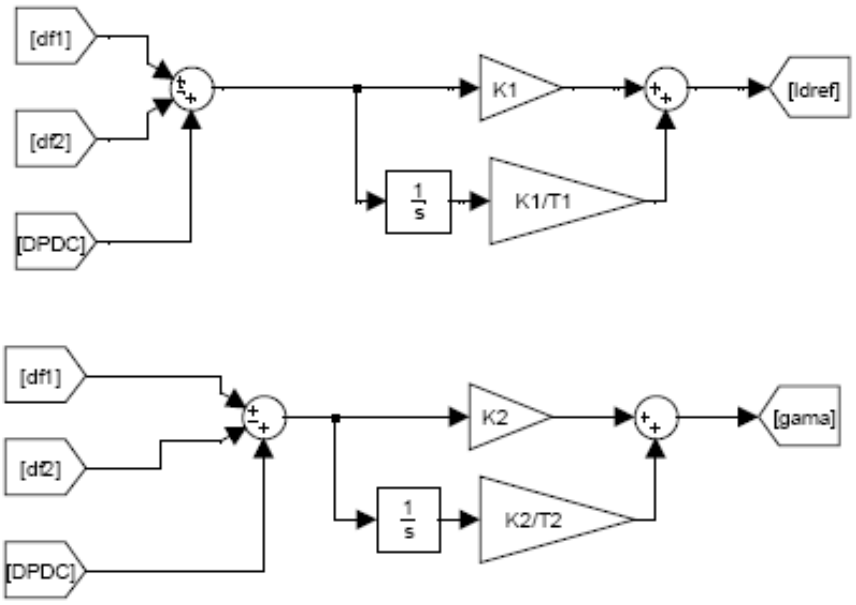

Fi8. 7. The designed PI controllers for adjusting the current source points and extinction angle.

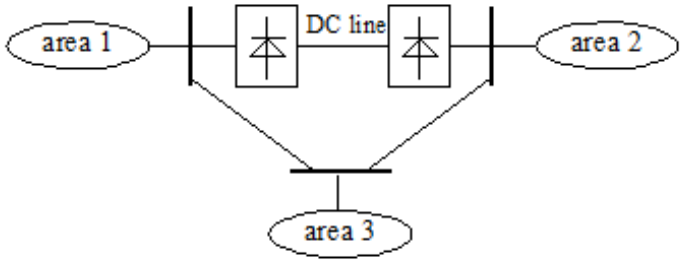

Fig. 8. Model of a three area network with DC interface line.

As a result, in order to control the system, current reference points and extinction angle is adjusted according to frequency error (f_1-f_2) with two PI controller as the following Fig. 7.

As it is seen, values of extinction angle and current source are obtained by passing frequency error and power error from PI controller. These values are used in controlling loops which have been explained previously.

To improve system performance, DC line control parameters, as well as PI controller coefficients, must be optimally selected. For this purpose, the coordination search optimization algorithm is introduced and applied.

3. HARMONY SEARCH ALGORITHM

HSA was invented first for optimizing the music quality [37,38]. It features several advantages including simple structure, the requirement of few parameters, rapid convergence and robustness [39,40]. This algorithm can be applied to different fields of research, owing to its ability to balance exploitation and exploration [41].

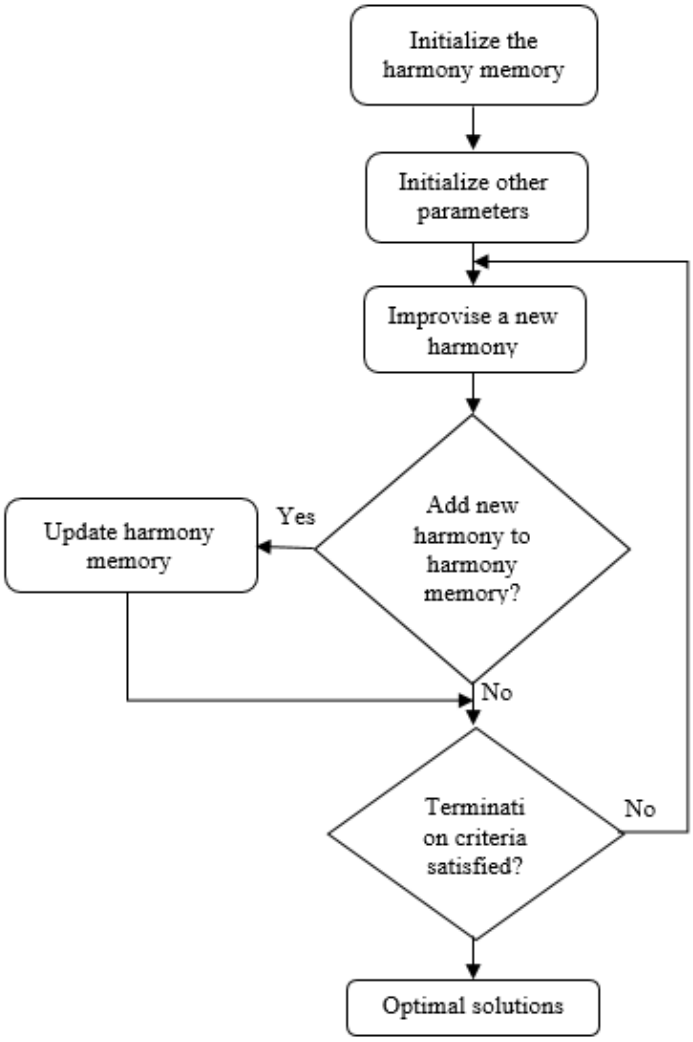

Fig. 9. Flow chart of harmony search algorithm for optimization.

Optimization processes of the objective function are performed in the following 5 stages:

First stage: determination of primary values and algorithm parameters. Generally, an optimization problem is stated as the following:

$$\min\{f(x)|x \in X\}, \quad st: (x) \geq 0, (x) = 0 \tag{11}$$

where x is a set of variables which are placed in f function and X is a set of values of xi. HSA parameters are: harmony memory size (HMS), harmony memory considering rate (HMCR), pitch adjusting rate (PAR), number of decision variables is (N) and number of repeats is (NI) which is the term of the same algorithm finishing. They are determined in this stage too.

Second stage: determination of primary values of harmony memory. In this stage, matrix harmony memory is filled by random

variables, it is necessary to say that dimensions of this matrix are HMS.

Third stage: optimization of harmonies. The new compound is formed according to the following three rules: consideration of harmony memory, adjusting the pitch size and random selection. Making a new compound is named optimization of harmony.

Fourth stage: variation of harmony memory. If new compound make the objective function value optimize more than previous harmony memory replies, they are replaced by the present values in harmony memory.

Fifth stage: investigation of algorithm finishing term. If the algorithm finishing term (most number of optimization) arrives, the calculations are stopped, and otherwise third and fourth stages are repeated.

The flow chart of HSA for optimization is shown in Fig. 8.

4. SIMULATION RESULTS

A model of load-frequency control has been represented in Fig. 9 for a three area network with the DC communication line and the system data have been shown in Table 1.

In this model, a small power system A (5100 MW) has been connected to a big power system B (25000) via DC interface line and a great power system C (30000) has been connected to areas A and B via two AC interface lines.

For the three area system, the objective function is considered according to the bellow equation:

$$\text{objective function} = \int_0^{T_{end}} [(\Delta f_1)^2 + (\Delta f_2)^2 + (\Delta f_3)^2 + (\Delta P_{DC})^2]\, t\, dt \quad (12)$$

Results from performing the harmony optimization algorithm are indicated in Table 2. In this section, the five modes of load change are examined according to Table 3. Frequency variations of controlling areas 1, 2 and 3 and variations of transmit power after applying disorder in the above all five modes are investigated and only variations of the first mode are presented in the following Figs. 10-15, respectively.

TABLE 1. ***Parameters of Three Area System.***

Parameters	symbols	System area 1	System area 2	System area 3
System capacity (MW)	-	5100	25000	30000
Generator inertia constant (MWs/Hz)	H	217	1064	1277
Load sensibility coefficient to frequency (MW/Hz)	D	204	1000	1200
Governor time constant	τ_g	2	2	2
Turbine time constant (sec)	τ_T	4	4	4
Adjustment coefficient (MW/Hz)	R	510	2500	3000

TABLE 2. ***Optimized Parameters of Three Area System.***

K_α	0.6	T_α	0.022	K_1	202.3	T_1	0.002
k_β	24	T_β	0.011	K_2	201.1	T_2	0.0034

TABLE 3. ***Areas Load Variations.***

No.	Load variations of area 1	Load variations of area 2	Load variations of area 3
First	100MW	-	-
Second	-	100MW	-
Third	-	-	100MW
Fourth	100MW	-100MW	-
Fifth	100MW	100MW	100MW

It is seen that steady-state frequency error with using the HVDC line is very lower than the mode without HVDC. For more investigation about the suggested system operation, the results of the simulation are summarized as in Table 4.

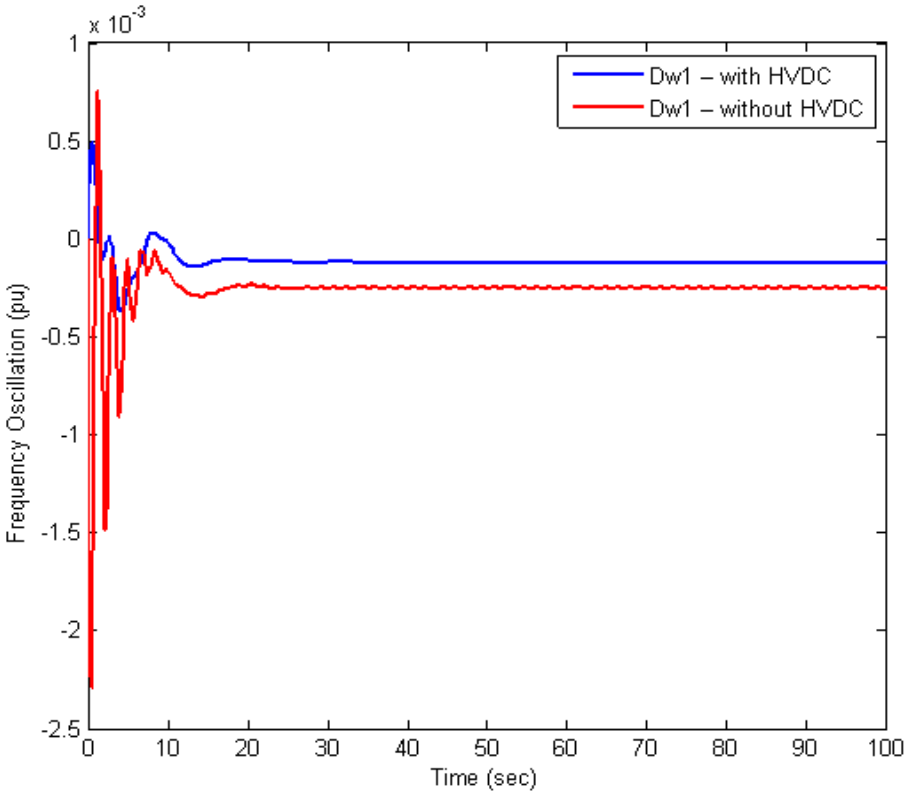

Fig. 10. Deviations of area-1 frequency for the first mode.

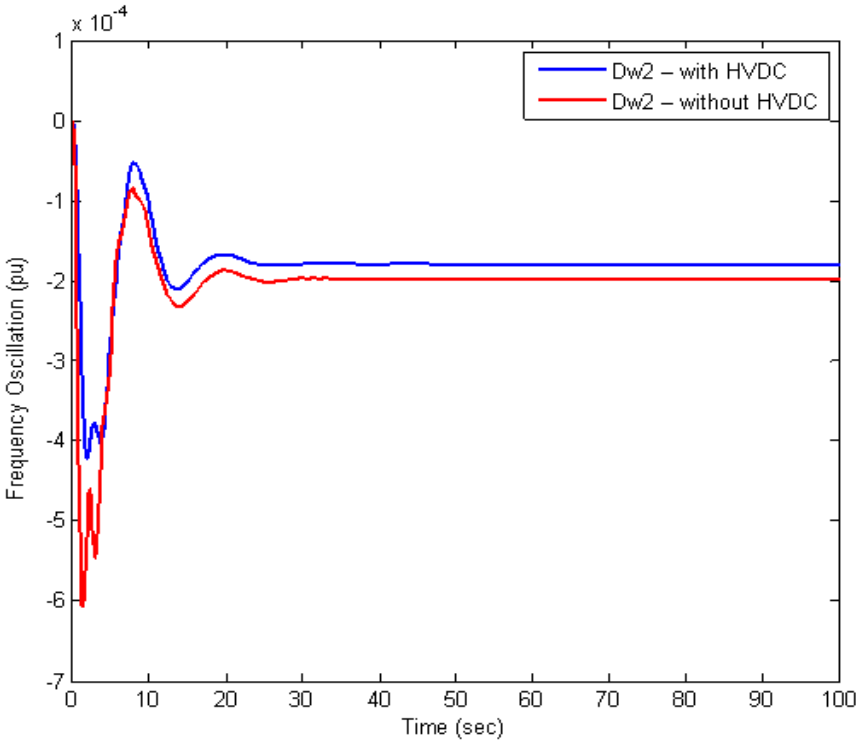

Fig. 11. Deviations of area 2 frequency for the first mode.

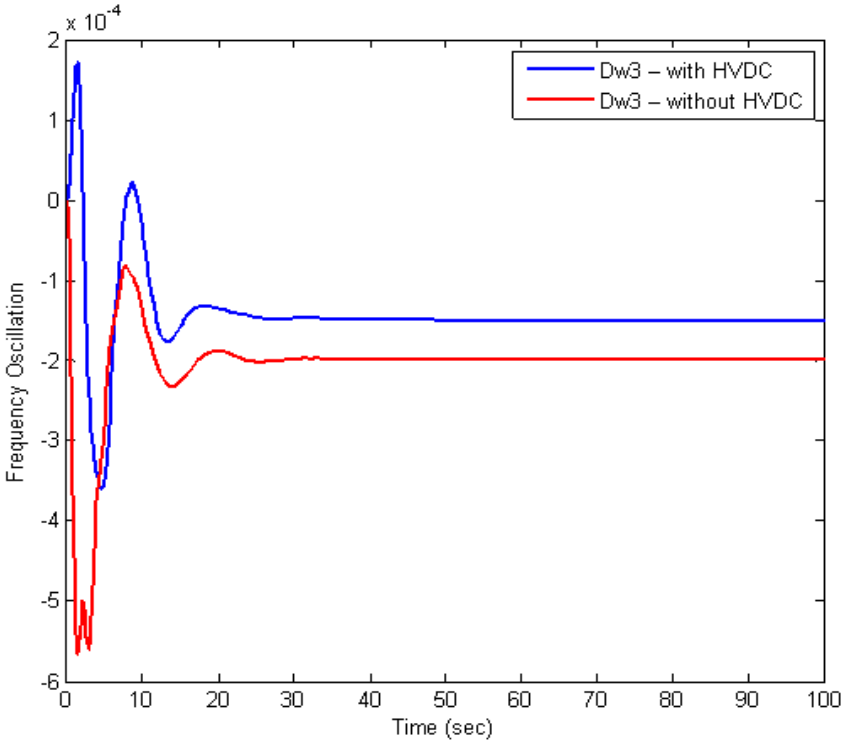

Fig. 12. Deviations of area 3 frequency for the first mode.

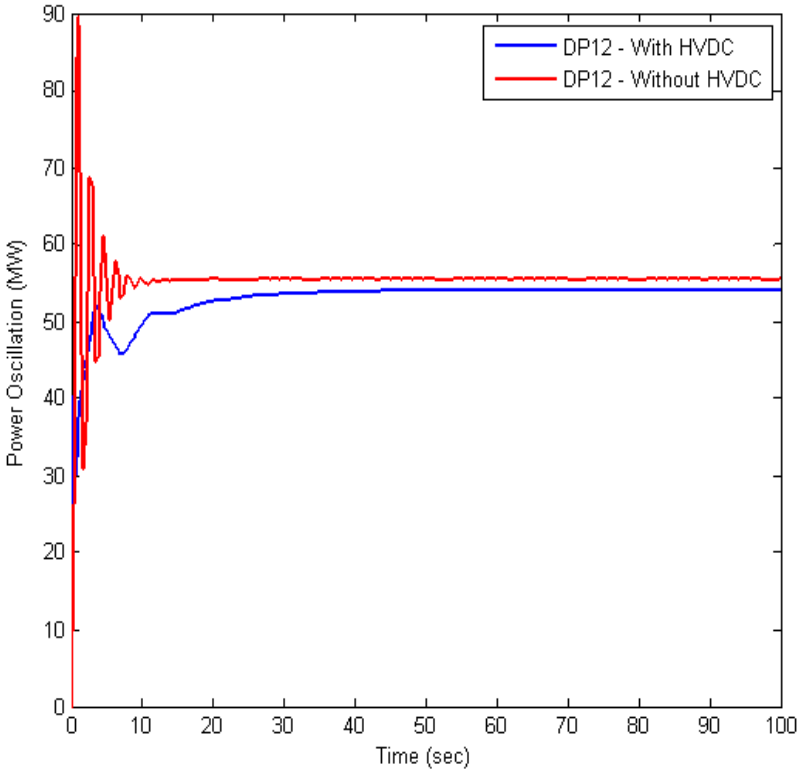

Fig. 13. DC line power between areas 1 and 2 for the first mode.

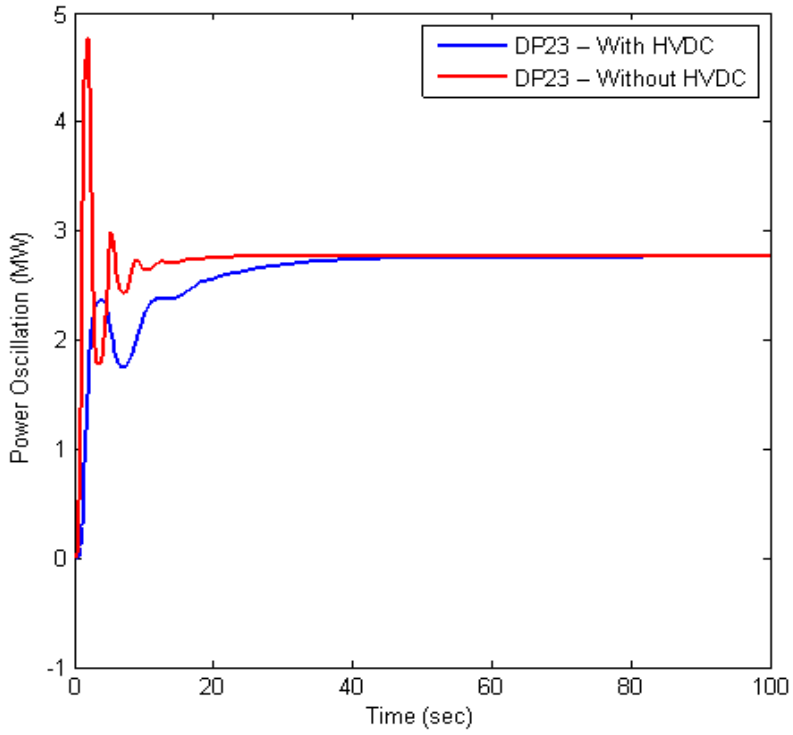

Fig. 14. Ac line power between areas 2 and 3 for the first mode.

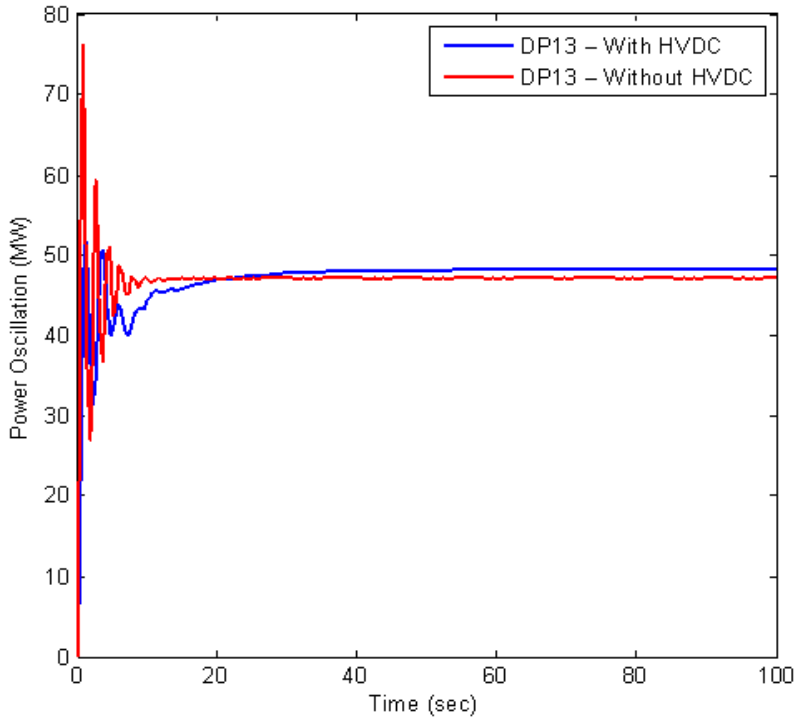

Fig. 15. AC line power between areas 1 and 3 for the first mode.

Table 4. ***Comparison of Results.***

Type of network	Mode	Description	Network with HVDC	Network without HVDC
Three area	First mode	Load increasing 100MW in area 1	$\Delta f_1 = -0.1\times10^{-3}$ $\Delta f_2 = -1.9\times10^{-4}$ $\Delta f_3 = -1.5\times10^{-3}$	$\Delta f_1 = -0.25\times10^{-3}$ $\Delta f_2 = -2.1\times10^{-4}$ $\Delta f_3 = -2\times10^{-3}$
	Second mode	Load increasing 100MW in area 2	$\Delta f_1 = -1\times10^{-4}$ $\Delta f_2 = -1.5\times10^{-4}$ $\Delta f_3 = -1.8\times10^{-4}$	$\Delta f_1 = -2\times10^{-4}$ $\Delta f_2 = -2\times10^{-4}$ $\Delta f_3 = -2\times10^{-4}$
	Third mode	Load increasing 100MW in area 3	$\Delta f_1 = -1\times10^{-4}$ $\Delta f_2 = -0.5\times10^{-4}$ $\Delta f_3 = -0.7\times10^{-4}$	$\Delta f_1 = -2\times10^{-4}$ $\Delta f_2 = -2\times10^{-4}$ $\Delta f_3 = -2\times10^{-4}$
	Fourth mode	Load increasing 100MW in area 1 and load decreasing in area 2	$\Delta f_1 = 0.1\times10^{-4}$ $\Delta f_2 = 0.1\times10^{-4}$ $\Delta f_3 = 0.1\times10^{-4}$	$\Delta f_1 = 4\times10^{-4}$ $\Delta f_2 = 4\times10^{-4}$ $\Delta f_3 = 4\times10^{-4}$
	Fifth mode	Load increasing 100MW in all three areas	$\Delta f_1 = -0.1\times10^{-3}$ $\Delta f_2 = -1.8\times10^{-4}$ $\Delta f_3 = -1.7\times10^{-4}$	$\Delta f_1 = -1.2\times10^{-3}$ $\Delta f_2 = -2\times10^{-4}$ $\Delta f_3 = -2\times10^{-4}$

5. CONCLUSION

A power system control is required to maintain a continuous balance between power generation and load demand. A solution is introduced for controlling the load-frequency in reconstructed systems, using HVDC lines is presented.

An analytical model of HVDC transmission system in controlling load-frequency are designed according to circuit and controlling equations by designing two PI controllers. The controlling parameters with HAS have been obtained in optimum value. The simulation results for power system with three-area in two modes with HVDC and without HVDC confirms that the suggested system has proper operation to reduce frequency error and power and frequency oscillations damping.

NOMENCLATURE

L_{dr} rectifier filter reactance
L_{di} inverter filter reactance
L_d half of reactance line resistance
R_d half of dc line resistance
V_{dr} dc voltage of rectifier
V_{di} dc voltage of inverter
I_{dr} dc current of rectifier
I_{di} dc current of inverter
C_{dc} grounding line capacitance
V_C grounding lined capacitance voltage
γ extinction angle
f(x) objective function
g(x) non-equivalence bond
h(x) equality bond function
I_d dc line current

ABBREVIATIONS

AGC Automatic generation control
AVR Automatic voltage regulator
CC Constant current
CEA Constant extinction angle
ESS Energy storage system
FACTS Flexible AC transmission systems
HAS Harmony search algorithm
HVDC High voltage direct current
LFC Load-frequency control
LFM Load frequency management
PID Proportional–integral–derivative
PSO Particle swarm optimization
SMC Sliding mode controller
TDC Transient droop compensator

REFERENCES

[1] R. Shahedi, K. Sabahi, M. Tayana, A. Hajizadeh, “Self-tuning fuzzy PID controller for load frequency control in ac microgrid with considering of input delay”, Journal of Intelligent Procedures in Electrical Technology, vol. 9, no. 35, pp. 19-26, Autumn 2019 (in Persian).

[2] E. Abbaspour, B. Fani, E. Heydarian-Forushani, “A bi-level multi agent based protection scheme for distribution networks with distributed generation”, International Journal of Electrical Power and Energy Systems, vol. 112, pp. 209-220, Nov. 2019.

[3] G. Shahgholian, J. Faiz, B. Fani, M. R. Yousefi, "Operation, modeling, control and applications of static synchronous compensator: A review", Proceeding of

the IEEE/IPEC, Singapore, pp. 596-601, Oct. 2010.

[4] S. Ebrahimi, A. Moghassemi, J. Olamaei, “PV inverters and modulation strategies: A review and a proposed control strategy for frequency and voltage regulation”, Signal Processing and Renewable Energy, vol. 4, no. 1, pp. 1-21, Winter 2020.

[5] G. Shahgholian, K. Khani, M. Moazzami, "The Impact of DFIG based wind turbines in power system load frequency control with hydro turbine", Journal of Iranian Dam and Hedroelectric, Vol. 1, No. 3, pp. 38-51, Winter 2015 (in Persian).

[6] M. F. Hassan, A. A. Abouelsoud, H. M. Soliman, "Constrained load-frequency control", Journal Electric Power Components and Systems, vol. 36, no. 3, pp. 266-279, 2008.

[7] D. H. Tungadio, Y. Sun, "Load frequency controllers considering renewable energy integration in power system", Energy Reports, Vol. 5, pp. 436–454, 2019.

[8] A. Pappachen, A. P. Fathima, "Load frequency control in deregulated power system integrated with SMES–TCPS combination using ANFIS controller", International Journal of Electrical Power and Energy Systems, Vol. 82, pp. 519-534, Nov. 2016.

[9] A. Latif, S. M. S. Hussain, D. C. Das, T. S. Ustun, “State-of-the-art of controllers and soft computing techniques for regulated load frequency management of single/multi-area traditional and renewable energy based power systems”, Applied Energy, vol. 266, Article Number: 114858, May 2020.

[10] A. Pappachen, A. P. Fathima, “Critical research areas on load frequency control issues in a deregulated power system: A state-of-the-art-of-review”, Renewable and Sustainable Energy Reviews, vol. 72, pp. 163-177, 2017.

[11] V. Gholamrezaie, M.G. Dozein, H. Monsef, B. Wu, "An optimal frequency control method through a dynamic load frequency control (LFC) model incorporating wind farm", IEEE Systems Journal, Vol. 12, No. 1, pp. 392-401, March 2018.

[12] E. J. Oliveira, L. M. Honorio, A. H. Anzai, L. W. Oliveira, E. B. Costa, "Optimal transient droop compensator and PID tuning for load frequency control in hydro power systems", International Journal of Electrical Power and Energy Systems, Vol. 68, pp. 345-355, June 2015.

[13] A. Hamidi, J. Beiza, T. Abedinzade, A. Daghigh, “Improving the dynamic stability of power grids including offshore wind farms and equipped with HVDC transmission system using adaptive neural controller”, Journal of Intelligent Procedures in Electrical Technology, vol. 11, no. 42, pp. 79-99, Summer 2020 (in Persian).

[14] Y. Phulpin, "Communication-free inertia and frequency control for wind generators connected by an HVDC-link", IEEE Trans. on Power Systems, Vol. 27, No. 2, pp. 1136-1137, May 2012.

[15] Y. Pipelzadeh, N.R. Chaudhuri, B. Chaudhuri, T.C. Green, "Coordinated

control of offshore wind farm and onshore hvdc converter for effective power oscillation damping", IEEE Trans. on Power Systems, vol. 32, no. 3, pp. 1860-1872, May 2017.

[16] M. Benasla, T.Allaoui, M. Brahami, V. K. Sood, M. Denaï, "Power system security enhancement by HVDC links using a closed-loop emergency control", Electric Power Systems Research, vol. 168, pp. 228-238, March 2019.

[17] L. Fan, Z. Miao, D. Osborn, "Wind farms with HVDC delivery in load frequency control", IEEE Trans. on Power Systems, vol. 24, no. 4, pp. 1894-1895, Nov. 2009.

[18] M. Tavakoli, E. Pouresmaeil, J. Adabi, R. Godina, J. P.S. Catalão, "Load-frequency control in a multi-source power system connected to wind farms through multi terminal HVDC systems", Computers and Operations Research, Vol. 96, pp. 305-315, Aug. 2018.

[19] E. Rakhshani, D. Remon, P. Rodriguez, "Effects of PLL and frequency measurements on LFC problem in multi-area HVDC interconnected systems", International Journal of Electrical Power and Energy Systems, Vol. 81, pp. 140-152, Oct. 2016.

[20] R. Shankar, S. R. Pradhan, K. Chatterjee, R. Mandal, "A comprehensive state of the art literature survey on LFC mechanism for power system", Renewable and Sustainable Energy Reviews, vol. 76, pp. 1185-1207, Sept. 2017.

[21] N. Pathak, A. Verma, T. S. Bhatti and I. Nasiruddin, "Modeling of HVDC tie links and their utilization in AGC/LFC operations of multiarea power systems", IEEE Trans. on Industrial Electronics, vol. 66, no. 3, pp. 2185-2197, March 2019.

[22] A. Khanjanzadeh, S. Soleymani, B. Mozafari, M. Fotuhi, "Integrated multi-area power system with HVDC tie-line to enhance load frequency control and automatic generation control", Electrical Engineering, vol. 102, pp. 1223–1239, 2020.

[23] G. Chen, Z. Li, Z. Zhang, S. Li, "An improved ACO algorithm optimized fuzzy PID controller for load frequency control in multi area interconnected power systems", IEEE Access, vol. 8, pp. 6429-6447, 2020.

[24] Y. Liu, K. Sun, "Solving power system differential algebraic equations using differential transformation", IEEE Trans. on Power Systems, vol. 35, no. 3, pp. 2289-2299, May 2020.

[25] E. Aghadavoodi, G. Shahgholian, "A new practical feed-forward cascade analyze for close loop identification of combustion control loop system through RANFIS and NARX", Applied Thermal Engineering, Vol. 133, pp. 381-395, March 2018.

[26] G. Shahgholian, K. Khani, M. Moazzami, "Frequency control in autanamous microgrid in the presence of DFIG based wind turbine", Journal of Intelligent Procedures in Electrical Technology, vol. 6, no. 23, pp. 3-12, Autumn 2015 (in Persian).

[27] G. Xu, J. Wang, C. Chen, "Feedback stabilization for ac/dc power system with nonlinear loads", Electric Power Systems Research, vol. 74, no. 5, pp. 247–255, May 2005.

[28] M. Ghasemi, A. Roosta, B. Fani, “Coordinated control of FACTS devices by using ADALINE neural network to enhance the transient stability of power system”, Journal of Intelligent Procedures in Electrical Technology, Vol. 3, No. 9, pp. 27-40, Spring 2012 (in Persian).

[29] Y. Yoshida, T. Machida, "Study of the effect of the dc Link on frequency control in interconnected ac systems", IEEE Trans. on Power Apparatus and Systems, Vol. 88, No. 7, pp. 1036-1042, 1999.

[30] Y. M. Alsmadi, V. Utkin, M. A. Haj-ahmed, L. Xu, "Sliding mode control of power converters: DC/DC converters", International Journal of Control, Vol. 91, no. 11, 2018.

[31] K. Sano, M. Takasaki, "A surgeless solid-state DC circuit breaker for voltage-source-converter-based HVDC systems", IEEE Trans. on Industry Applications, Vol. 50, No. 4, pp. 2690-2699, 2014.

[32] H. Wu, M. Han, K. Sun, "Dual-voltage-rectifier-based single-phase ac–dc converters with dual dc bus and voltage-sigma architecture for variable dc output applications", IEEE Trans. on Power Electronics, vol. 34, no. 5, pp. 4208-4222, May 2019.

[33] S. Aldhaher, D. C. Yates, P. D. Mitch-eson, "Load-independent class E/EF inverters and rectifiers for mhz-switching applications", IEEE Trans. on Power Electronics, vol. 33, no. 10, pp. 8270-8287, Oct. 2018.

[34] L. Hong, X. Zhou, Y. Liu, H. Xia, H. Yin, Y. Chen, L. Zhou, Q. Xu, "Analysis and improvement of the multiple controller interaction in LCC-HVDC for mitigating repetitive commutation failure", IEEE Trans. on Power Delivery, Early Access Article.

[35] N. Yousefpoor, A. Narwal, S. Bhatt-acharya, "Control of dc-fault-resilient voltage source converter-based HVDC transmission system under dc fault operating condition", IEEE Trans. on Industry Applications, Vol. 62, No. 6, pp. 2690-2699, 2015.

[36] L. W. Sheng, A. Razani, N. Prabhakaran, "Control of high voltage direct current (HVDC) bridges for power transmission systems", Proceeding of the IEEE/SCOReD, pp. 430-435, Putrajaya, Dec. 2010.

[37] M. Mahdavi, M. Fesanghary, E. Dama-ngir, “An improved harmony search algorithm for solving optimization problems”, Journal of Applied Mathematics and Computation, Vol. 188, pp.1567–1579, 2007.

[38] F. Zhao, S. Qin, G. Yang, W. Ma, C. Zhang, H. Song, "A differential-based harmony search algorithm with variable neighborhood search for job shop scheduling problem and its runtime analysis", IEEE Access, vol. 6, pp. 76313-76330, 2018.

[39] T. Zhang, X. Xu, Z. Li, A. Abu-Siada, Y. Guo, "Optimum location and para-meter setting of STATCOM based on

improved differential evolution harmony search algorithm", IEEE Access, vol. 8, pp. 87810-87819, 2020.

[40] M. N. Ambia, H. M. Hasanien, A. Al-Durra, S. M. Muyeen, "Harmony search algorithm-based controller parameters optimization for a distributed-generation system", IEEE Trans. on Power Delivery, vol. 30, no. 1, pp. 246-255, Feb. 2015.

[41] A. A. Al-Omoush, A. A. Alsewari, H. S. Alamri, K. Z. Zamli, "Comprehensive review of the development of the harmony search algorithm and its applications", IEEE Access, vol. 7, pp. 14233-14245, Jan. 2019